



저작자표시-비영리-변경금지 2.0 대한민국

이용자는 아래의 조건을 따르는 경우에 한하여 자유롭게

- 이 저작물을 복제, 배포, 전송, 전시, 공연 및 방송할 수 있습니다.

다음과 같은 조건을 따라야 합니다:



저작자표시. 귀하는 원저작자를 표시하여야 합니다.



비영리. 귀하는 이 저작물을 영리 목적으로 이용할 수 없습니다.



변경금지. 귀하는 이 저작물을 개작, 변형 또는 가공할 수 없습니다.

- 귀하는, 이 저작물의 재이용이나 배포의 경우, 이 저작물에 적용된 이용허락조건을 명확하게 나타내어야 합니다.
- 저작권자로부터 별도의 허가를 받으면 이러한 조건들은 적용되지 않습니다.

저작권법에 따른 이용자의 권리는 위의 내용에 의하여 영향을 받지 않습니다.

이것은 [이용허락규약\(Legal Code\)](#)을 이해하기 쉽게 요약한 것입니다.

[Disclaimer](#)

Master of Science

A new *Caenorhabditis elegans* AP endonuclease engaged in rescue from replication stress-induced arrest

The Graduate school of University of Ulsan,
Department of Life Science,
Pham Thi Hoa

A new *Caenorhabditis elegans* AP endonuclease engaged in rescue from replication stress-induced arrest

Supervisor: Professor Ahn Byungchan

This dissertation is submitted to University of Ulsan in partial fulfillment of the requirements for the degree of Master of Science in Life science

by

Pham Thi Hoa

Department of Life Science

University of Ulsan

July, 2020

University of Ulsan
Department of Life Science,

This dissertation, “A new *Caenorhabditis elegans* AP endonuclease engaged in rescue from replication stress-induced arrest” is hereby approved in partial fulfillment of the requirements for the degree of Master of Science

Committee Chair: Professor Choi Kee-Ryong

Committee member: Professor Back Sung-Hoon

Committee member: Professor Ahn Byungchan

Contents

I.	List of Figures.....	5
II.	Acknowledgement.....	6
III.	Abstracts.....	7
IV.	Introductions.....	8
V.	Materials and methods.....	10
VI.	Results.....	14
VII.	Discussion.....	35
VIII.	References.....	38

List of figures

1. Table 1. List of oligomers	19
2. Figure 1. Purification of Recombinant EXD-3 protein.	20
3. Figure 2. Enzyme activity of EXD-3.	21
4. Figure 3. Nicking activity of EXD-3 on a natural abasic site.	22
5. Figure 4. Embryonic survival of <i>exd-3(tm2546)</i> .	23
6. Figure 5. Recovery from cell cycle arrest post HU-treatment.	26
7. Figure 6. Recovery from cell cycle arrest post CPT-treatment.	28
8. Figure 7. <i>exd-3(tm2546)</i> worms respond to HU-induced DNA damage.	30
9. Figure 8. <i>exd-3(tm2546)</i> worms respond to CPT-induced DNA damage.	32
10. Figure 9. Formation of EXD-3 foci after HU treatment.	34

Acknowledgement

First of all, I would like to express my most sincere gratitude to my supervisor, doctor Ahn ByungChan. Thank you so much for all you have done for me. You not only supported, taught, helped but also encouraged me a lot during my master course. Without your patient supporting, this thesis will never be done.

Besides that, I would also like to thank my beloved lab-mate, doctor Choi SeoYun, who have guided me and given me many tips in doing experiment as soon as I joined the Molecular Biology Genetic laboratory (MBG lab).

It is impossible not to mention my dear friends in Korea, Xuan Loan Doan, Tan Lien Pham, Thi Thom Nguyen, who shared with me all my joys and sorrows. Thank you for giving me the best memories that I can treasure from the rest of my life.

In particular, thank you my boyfriend, Thai Truong Bui, thank you for coming into my life and giving me joys, loving me, believing in me and always beside me even many up and down in my life.

Last but not least, I really appreciate my parents, my family who have always accompanied me, encouraged me, supported me without any requirements.

Thank you everyone, thank you for being an important piece of my life. All of you give me reason to overcome so many challenges, to improve myself day by day.

Korea, 2020 July.

Abstract

Apurinic/aprimidinic (AP) sites are one of the most frequent spontaneous lesions in DNA. They are highly mutagenic and lethal lesions that can inhibit transcription and DNA replication. AP sites are primarily repaired by the base excision repair (BER) pathway which is initiated by one of the two AP endonucleases. Organisms encode for evolutionarily conserved repair machinery, including specific AP endonuclease which incises the DNA backbone 5' to the AP site to undergo further DNA repair synthesis. We report on a new protein (EXD-3) from *Caenorhabditis elegans*, a putative exonuclease containing a domain homologous to human EXD3 and human Werner syndrome RNaseD, possesses endo- and exonuclease activities against abasic site. *exd-3* mutants are defected in recovery from replication stress-induced cell cycle arrest and the formation of EXD-3 foci is induced by various treatments that produce double-strand breaks. Thus, EXD-3 enables to perform recognition and incision at AP sites, and further restoration (repair) of replication stress-induced damage.

Introduction

Base excision repair (BER) corrects DNA bases damaged by oxidation, alkylation, and deamination. BER is well conserved in many organisms from *E. coli* to humans [1]. BER pathway is initiated by DNA glycosylases, which excise damaged or misincorporated bases. Base excision from DNA strand produces an apurinic/apyrimidinic (AP) site. In next step, AP endonucleases cleave the DNA backbone next to the AP site, creating a nick. The remaining abasic sugar is removed by a deoxyribo-phosphodiesterase, leaving a single nucleotide gap. Finally, DNA polymerase inserts the correct nucleotide and the remaining nick is sealed by a DNA ligase.

Besides AP sites of BER intermediates, AP sites are alternatively generated by spontaneous depurination/depyrimination[2;3] and are highly mutagenic lesions due to noncoding. Therefore, AP sites must be eliminated and corrected[4-6]. Correcting AP sites is initiated by incision with AP endonucleases. There are two families of AP endonucleases in living organisms; endonuclease IV (EndoIV) and exonuclease III (ExoIII) families[7;8]. *E. coli* exonuclease III was first identified and the Exo III homolog is present in all kingdoms of life, named APN2 in *Saccharomyces cerevisiae* and APE1 and APE2 in humans. The enzymes in this family are Mg^{2+} -dependent and are able to perform a wide variety of excision and incision reactions on DNA substrates, including AP endonuclease, 3'-5' exonuclease, 3'-dRpase and 3'-phosphatase, and occasionally nonspecific DNase activities[9]. *E. coli* endonuclease IV was identified from mutants lacking ExoIII and the endo IV homolog, APN1, exists in lower organisms but are absent in some groups, such as mammals and plants. The enzymes in this family are Zn^{2+} -dependent and also perform incision and excision reactions by AP endonuclease, 3'-5' exonuclease and 3'-dRpase. Hydrolytic AP endonucleases cleave the DNA phosphodiester bond 5' to the AP site to produce a 3'-hydroxyl group and a 5'-deoxyribose phosphate[10].

Unlike other multicellular eukaryotes, BER in the nematode species *Caenorhabditis elegans* (*C. elegans*) has not been well characterized and there are relatively few publications on BER in this organism. Two glycosylases[11-13] and two AP endonucleases[14;15] have been identified, and have been characterized biochemically[14;16;17]. The identified AP

endonucleases are EXO-3 (homologous to *Escherichia coli* Exo III) and APN-1 (homologous to *E. coli* Endo IV) [14;15;18]. EXO-3 has an Mg²⁺-dependent AP endonuclease and shows no significant level of a 3' to 5' exonuclease activity following incision at AP sites. APN-1 possesses a Zn²⁺-AP endonuclease and a 3'-diesterase and displays a 3' to 5'-exonuclease activity.

Even though organisms as *E.coli* and *Saccharomyces cerevisiae* have ExoIII and EndoIV, others as *Neisseria meningitidis* and human cells contain two AP endonucleases belonging to only the Exo III family [19;20] and no Endo IV homolog. The *Arabidopsis* genome encodes only three AP endonuclease homologs of ExoIII: APE1L, ARP, and AtAPE2 [21]. Rarely, *Bacillus subtilis* polymerase, PolX_{Bs}, shows an AP endonuclease activity to which exonuclease is linked genetically [22]. Surprisingly, a novel AP endonuclease involved in responding to DNA strand break was identified in humans [23]. Thus, we searched genes containing a 3-5 exonuclease domain from *C. elegans* genome database. A few genes were revealed and cloned, and their gene products were expressed in *E. coli*. Among them, *exd-3* gene contains a domain similar a human EXD3 (exonuclease 3'-5' domain containing 3) homology or human WRN exonuclease domain.

Here, we found that *exd-3* gene product has Mg²⁺-dependent AP endonuclease and a 3'-5' exonuclease and that EXD-3 protein forms foci in response to replication fork-associated DNA damage.

MATERIALS AND METHODS

1. Bacterial Strains and C. elegans

E. coli laboratory strain DH5 α (used for amplification of plasmids) and BL21AI (used for protein expression) were maintained on Luria Broth (LB) agar plates.

Unless otherwise indicated, nematodes were maintained and propagated at 20°C on nematode growth medium (NGM) plates and fed with *Escherichia coli* OP50 bacteria. Experiments were performed at 20°C on young adult hermaphrodites. Bristol (N2) as wild-type and *C. elegans* *exd-3(tm2546)* mutants was obtained from the National BioResource Project (Tokyo, Japan).

2. Proteins and antibodies

E. coli endonuclease IV and uracil DNA glycosylase were purchased from New England Biolabs (MA USA). A monoclonal anti-GST antibody was purchased from Ab Frontiers (Korea). The EXD-3 antibody was prepared by antipeptide antibody production. Two polypeptides derived from Peptide 1 (1st~21st; MGDTTSSSEDVPE NKQKSLKFE-C) and Peptide 3 (273rd~295th; KFFNGQVKQFKFDLEERRDAPKF-C) were selected and the polyclonal antipeptide antibody was produced from rabbits (Ab Frontiers, Korea) and further purified by Protein A column. Anti-RPA-1 antibody was produced from mouse [24].

3. Construction of the aGST-Fusion Protein

C. elegans *exd-3* ORF clone (2353 nucleotide; Catalog#: OCE1182-202134345, Open Biosystems) was used to amplify with the primers (Forward primer: 5'–CACC ATG GGA GAT ACA ACA TCA TCG–3'; Reverse primer: 5'–TTA ACA ATT CAA TTT AAT ATA ATC TTG ATC TGG–3') designed for the pENTR/D/TOPO plasmid (Invitrogen, USA) and Pfu DNA polymerase (Stratagene, USA). The cloned EXD-3 in pENTR/D/TOPO was transferred to the *E. coli* expression vector pDEST15 for GST-fusion protein using the Gateway LR Clonase II (Invitrogen, USA) and confirmed by DNA sequencing (data not shown). The pDEST15 containing EXD-3 was transformed into *E. coli* BL21AI for protein expression.

4. Purification of GST-Fusion Proteins

The recombinant GST-EXD-3 protein was expressed in *E. coli* BL21AI. *E. coli* cells were grown at 37°C in 1 liter of LB media containing 100 µg/ml ampicillin to an OD₆₀₀ of 0.4. L-arabinose (Sigma-Aldrich, USA) was added to the culture to a final concentration of 0.2% (w/v) to induce protein production, and the cells were grown overnight at 22°C. Cultured cells were harvested by centrifugation, suspended in 20 ml lysis buffer (50 mM Tris-HCl, pH 8.0, 500 mM NaCl, 0.5 mM EDTA, 5 mM β-mercaptoethanol, 10% glycerol, 1 mM PMSF, 1 protease inhibitor cocktail tablet (Roche, Mannheim, Germany) and lysed by sonication (duty cycle 20/output 2, 10 bursts at 10 second intervals, Branson). Lysates were clarified by centrifugation at 10,000×g for 30 minutes at 4°C. The lysate was loaded into GSTrap chromatography column (1 ml, Amersham, USA). The column was washed with 10 column volumes of wash buffer 1 (50 mM Tris-HCl at pH 8.0, 200 mM NaCl, 5 mM DTT, 10% glycerol,) and 10 column volumes of wash buffer 2 (50 mM Tris-HCl at pH 8.0, 50 mM NaCl, 5 mM DTT, 10% glycerol) to remove nonspecifically bound protein. GST-EXD-3 was eluted with 5 ml of elution buffer (50 mM Tris-HCl at pH 8.0, 50 mM NaCl, 5 mM DTT, 10% glycerol 1 mM glutathione, second elution with 5 mM glutathione). Peak fractions containing GST-EXD-3 were detected by a SDS-PAGE. Protein concentrations were determined by a Bio-Rad assay with BSA as the standard.

5. 3'-5' exonuclease EXD-3 has AP endonuclease activity

5.1 Oligonucleotide Substrates

Oligonucleotides were synthesized by IDT (Integrated DNA Technology, USA) and are listed in Table S1. A single oligonucleotide was labeled at the 5'-end with [γ -³²P] ATP (IZOTOP, Hungary). Oligonucleotides were incubated with T4 polynucleotide kinase (New England Biolabs, USA) for 1 hour at 37°C, followed by heat-inactivation for 10 minutes at 95°C. The labeled oligonucleotides were purified using G-25 Sepharose spin columns and annealed to unlabeled complementary strands. A synthetic 24-mer oligonucleotide with a uracil at position 14 and a complementary strand containing G opposite to U was synthesized by Bioneer (Korea). A synthetic 24-mer oligonucleotide with a Tetrahydrofuran (THF) lesion at position 12 and a complementary strand containing A opposite to THF was synthesized by Bioneer (Korea). DNA substrates for incision assays were annealed (Table 1).

5.2 Enzyme activity of EXD-3

For the AP endonuclease, DNA substrates were incubated with proteins in 15 μ l (final volume) of buffer (40 mM Tris-Cl at pH 8.0, 5 mM DTT, 4 mM MgCl₂, 0.1 mg/ml BSA, 10% glycerol) at 37°C for indicated times. Reactions for THF-AP substrate were stopped with 15 μ l formamide loading buffer (95% deionized formamide, 0.025% bromophenol blue, 0.025% xylene cyanole, and 10 mM EDTA). Samples were heated at 95°C for 5 min. Reaction for dU-G substrates was incubated UDG followed by heating at 55°C for 10 min. Then, EXD-3 or Endo IV was incubated at 37°C for the indicated times, stopped and heated at 55°C for 10 min before loading onto gels. Reaction products were separated by 8 M urea-17% polyacrylamide gel electrophoresis and viewed by autoradiography.

And for EXD-3 (E452A) (THF-AP DNA substrate was incubated in 10 μ l (final volume) of buffer (40 mM Tris-Cl at pH 8.0, 5 mM DTT, 4 mM MgCl₂, 0.1 mg/ml BSA, 10% glycerol) at 37°C with increasing concentration of protein (16, 32, 64 nM) for 20 min.

For the exonuclease, instead of THF- substrate, 5' overhang DNA substrate was used. Reactions were stopped with 10 μ l formamide loading buffer (95% deionized formamide). Samples were heated at 95°C for 5 min. Reaction products were separated by 8 M urea-18% polyacrylamide gel electrophoresis and viewed by autoradiography.

6. Measurement of embryonic survival

6.1 Embryonic survival post Hydroxyurea (HU) treatment

Ten L4-stage animals were grown on NGM plates containing indicated concentration of HU at 20°C for 16 h. And then transferred to HU-free plates with *Escherichia coli* OP50 and let worms lay eggs at 20°C. After 3-4 h, removing worms, the number of total laid eggs was counted. And post 24 h, the number of unhatched eggs was counted. The embryonic survival percentage was calculated by dividing the number of hatched eggs by the total number of laid eggs.

6.2 Embryonic survival post exposed to Camptothecin (CPT)

Post 24 hours exposed to NGM plates containing 0, 5, 10, 20, 40 μM CPT, ten L4-stage worms were transferred to CPT-free plates with *E. coli* OP50, where embryos were laid for 3-4 h. And the embryonic survival percentage is quantified as above mentioned with HU treatment.

7. Recovery ability post genotoxicity treatment.

L4 stage animals were placed into a new NGM plate containing 25 mM HU and treated for 6 h or 16 h. And then treated worms were transfer to HU-free plate to let them recovery. And then gonads were dissected at the indicated times (0, 6, 12, 24 h) after HU treatment and 4,6-diamidino-2-phenylindole (DAPI, 1 $\mu\text{g}/\text{ml}$) staining was performed. The stained gonads were observed with a Carl Zeiss Axioskop fluorescence microscope.

Also, 40 μM CPT treatment was performed with step by step as above mentioned of HU treatment but exposure times are 6 h and 24 h, respectively.

8. Immunostaining

Worms were dissected in egg salt buffer supplemented with 0.2 mM levamisol (Sigma-Aldrich, USA). Gonads were fixed in 2% paraformaldehyde for 5 min at room temperature followed by Post-fixation with 100% methanol at -20°C . Gonads were treated in PBSTx (PBS +0.1% Triton-X) for permeablization followed by washing with PBST (PBS +0.1% Tween 20). Blocking was performed by incubating the samples in PBSTB (PBST +0.5% BSA) for 30 min. Primary antibodies were diluted in PBSTB (anti-RPA-1 antibody (1:1000 dilution); anit-EXD-3 antibody (1:1000 dilution)) and allowed to bind at 4°C overnight in a humid chamber. Samples were washed three times for 10 min in PBST. Binding of secondary antibodies was performed for 2 h at room temperature with Alexa Fluor-conjugated goat anti-rabbit secondary antibodies, or Alexa Fluor-conjugated goat anti-mouse secondary antibodies (used in a 1:2000 dilution, Molecular probes) and washed three times for 10 min in PBST. After staining with DAPI (4,6-diamidino-2-phenylindole, 1 $\mu\text{g}/\text{ml}$), the gonads were mounted on 1% agarose pads and observed under an epifluorescence microscope (Carl Zeiss *Axioskop2 plus*).

Results

Purification of EXD-3 protein

The EST clone containing the full length of *C. elegans exd-3* gene was fused with an N-terminal GST-tag, expressed in *E. coli*, and purified using a GSTrap affinity column to approximately 95% homogeneity (Figure 1A). The recombinant protein has a molecular mass of 110 kDa (26.9 kDa GST + 91.2 kDa EXD-3) and migrated at ~120 kDa on a 7% polyacrylamide gel. Western blot analyses of the purified EXD-3 using a polyclonal anti-EXD-3 antibody and a monoclonal anti-GST antibody revealed a single band at ~120 kDa (Figure 1B).

One conserved glutamic acid 452 residue in EXD-3 corresponds to glutamic acid residue 84 in human WRN exonuclease domain, for the 3' → 5' exonuclease activity of human WRN[25]. We replaced the glutamic acid residue (E452A) of EXD-3 with an alanine residue. EXD-3(E452A) proteins were purified in a manner identical to that of the wild-type EXD-3 protein (data not shown).

EXD-3 incises AP site

Some 3'–5' exonucleases are associated with other enzymatic activities, such as polymerase or AP endonuclease. To monitor AP endonuclease activity of EXD-3, a duplex DNA oligonucleotide containing an internal tetrahydrofuran (THF), a stable analogue that mimics reduced AP site, was used (Figure 2A, Table 1). As a control of the possibility of THF to be recognized as AP site, this substrate was incubated in parallel with *E. coli* endonuclease IV (Endo IV), which is known to break the phosphodiester bond at the 5' side of THF-AP site[26]. The expected 11-mer product was produced (Figure 2A, lane 7). When purified WT EXD-3 was incubated with the substrate, incision at THF-AP site was detected (Figure 2A, lanes 2-6). In addition, there is one band below the 11-mer band at the incised AP site, which presumably resulted from 3'–5' exonucleolytic degradation of the incised AP site. The cleavage of the substrate at the 5' side of THF-AP site was observed in a protein concentration-dependent manner (Figure 2A, lanes 2-6) and the incision was linear with increasing concentrations (Figure 2B). In a time-course experiment, THF incision activity was analyzed

over time intervals during 20 min (Figure 2C, lanes 2-6). The product formation was linear over the time points monitored.

We further showed that the mutant EXD-3 (E452A) did incise THF-AP substrates (Figure 2D) digested 3'-recessed DNA (Figure 2E). The expected 11-mer product was produced (Figure 2D, lane 2). When the purified mutant EXD-3 (E452A) were incubated, incision at THF-AP site was detected (Figure 2D, lane 3-5).

In addition, to further confirm the 3'-5' exonuclease activity of mutant EXD-3 (E452A), we used a 5' overhang DNA substrate. There are some bands below the 24-mer band. The cleavage of the substrate at the end of 3' side of DNA substrate was observed in a protein concentration-dependent manner (Figure 2E, lane 2-4). In contrast, no band below the 24-mer band was detected with *E. coli* endonuclease IV (Endo IV) (Figure 2E, lane 5).

AP endonuclease incision of natural abasic site

We next tested whether EXD-3 cleaves natural a basic site. For this test, double-stranded 24-mer oligonucleotide containing a centrally placed dU-G base pair has been employed as a substrate for AP endonuclease assay (Figure 3, table 1). The substrate was treated with *E. coli* uracil DNA glycosylase (UDG), which removes uracil base, leaving AP site in DNA [27]. The resulting AP site is cleaved by AP endonuclease, *E. coli* endonuclease IV, producing a 13-mer product (Figure 3, lane 8).

When purified EXD-3 was incubated with UDG-treated DNA over time intervals, incision at AP site was detected (Figure 3, lanes 3-7). In addition, there is one dominant band below 13-mer, which presumably resulted from the exonuclease activity of EXD-3 on the incised AP site (Figure 3, lanes 3-7), similar to the band detected in THF-AP substrate (Figure 2). As a control, EXD-3 did not incise dU-G contained substrate in the absence of UDG (data not shown). This result suggests that EXD-3 can enter and incise natural AP site following action of a DNA glycosylase.

***exd-3(tm2546)* mutants are sensitive to HU and CPT**

Ten L4-stage animals were transferred to NGM plates containing indicated concentration of HU at 20°C for 16 h. And then the worms were placed on HU-free NGM plates to lay eggs (200-300 eggs) for 2-3 h. The embryonic survival percentage was calculated by dividing the

number of hatched eggs by the total number of laid eggs. Compared to N2 wild-type worms, the embryo survival of *exd-3(tm2546)* mutant was more sensitive to HU but not much (Figure 4A). For example, at 5 mM HU around 98% embryo can be survival in both N2 wild-type and *exd-3(tm2546)* worms, whereas 23% embryonic survival *exd-3(tm2546)* worms but 37% embryonic survival N2 worms at 25 mM HU.

Also, *exd-3(tm2546)* mutants were sensitive to CPT (Figure 4B). The embryonic survival of *exd-3(tm2546)* mutants were reduced compared to that of N2 worms. For example, 6% embryonic survival *exd-3(tm2546)* worms but 27% embryonic survival N2 worms at 40 μ M CPT, five-fold difference.

Recovery from a replication stress-induced cell cycle arrest

The *C. elegans* hermaphrodite germline is a useful model for studying DNA damage response. Exposure of worms to DNA damaging agents, such as hydroxyurea (HU), Camptothecin (CPT), or ionizing radiation causes a transient halt in cell cycle progression in the mitotically proliferating zone [28]. The cell cycle arrest leads to a decreased number of mitotic germ cells and enlarged mitotic germ cells since cellular and nuclear growth continues to occur [29]. Short HU treatments, a drug depleting deoxynucleoside triphosphate pools, result in stalled replication forks that retain the ability to restart for some time before inactivated, whereas prolonged treatments lead stalled replication forks to be processed into collapsed forks, a form of DSBs that are repaired by recombination process.

The cell cycle arrest leads to a decreased number of mitotic germ cells and enlarged mitotic germ cells since cellular and nuclear growth continues to occur [28]. Short HU treatments, a drug depleting deoxynucleoside triphosphate pools, result in stalled replication forks that retain the ability to restart for some time before inactivated, whereas prolonged treatments lead stalled replication forks to be processed into collapsed forks, a form of DSBs that are repaired by recombination process.

We analyzed cell cycle arrest and recovery from the arrest after exposure to HU and CPT. After treatment of L4-stage *C. elegans* with CPT or HU and observation the morphologies of DAPI-stained mitotic germline nuclei, wild-type N2 worms transiently stopped nuclei dividing after 6-h HU treatment as revealed by enlarged mitotic nuclei (Figure 5A, no HU).

Cell cycle arrest was also evident in *exd-3(tm2546)* mutants (Figure 5A). These cell cycle arrest morphologies are observed more clearly after 16-h exposure to HU in both N2 wild-type and *exd-3(tm2546)* mutants (Figure 5B). All results indicate that *exd-3(tm2546)* mutants have a normal S-phase checkpoint to induce cell cycle arrest. The number of germline cell and size of each cell are almost normalized to untreated worms, and no difference between wild-type N2 and *exd-3(tm2546)* worms (Figure 5A). This data showed that post 6-h exposure to HU, both wild-type N2 and *exd-3(tm2546)* worms completely recovered after 18-h. But in case 16-h exposure to HU, wild-type N2 germline nuclei, HU-induced cell cycle arrest appeared to be reversible since the volume of the nuclei gradually decreased over times (from 58 to 15 germline nuclei cell in 50 x 20 μm in tip cells of untreated and treated worm, respectively) and the number gradually increased by 24 h after removal from HU (up to 45 nuclei cell in 50 x 20 μm in tip cells) (Figure 5B, 24 h post HU-treatment). In contrast, germ cells in *exd-3(tm2546)* failed to reverse to those in HU-free worms (Figure 5B, 24 h post HU-treatment). The number of mitotic germ cells change from 56 in untreated worm to 20 in treated worm and finally 19 in worm at 24 h after removal from HU. This result indicates that EXD-3 somehow is involved in the recovery from cell cycle arrest.

Additionally, a response of N2 and *exd-3(tm2546)* mutant to CPT is strongly same as HU. Wild-type N2 and *exd-3(tm2546)* worms showed enlarged germ cells (Figure 6A, 0h post 24h CPT treatment), indicating that cell cycle arrest was normally induced by the CPT (40 μM) after 6 h (Figure 6A). To investigate recovery from CPT-induced cell cycle arrest, worms were transferred to CPT-free plates and analyzed mitotic nuclei dividing and volume. N2 showed increased number of mitotic nuclei, reaching to that in CPT-free worms (Figure 6B, 24 h post CPT-treatment). However, nuclei division was delayed in *exd-3(tm2546)* worms compared to the size and number of CPT-free nuclei (Figure 6B, post CPT-treatment), indicating that recovery from cell cycle arrest induced by prolonged CPT exposure is failed. Whereas *exd-3(tm2546)* worms were exposed for short CPT blocks, the size of the nuclei decreased and the number gradually increased by 18 h after removal from CPT, approximately 80% normalized to untreated worms.

Response to replication stress-induced DNA damage

HU leads to replication fork stalling and single strand regions at the stalled replication forks induce accumulation of replication protein A (RPA) which recruits DNA damage checkpoint activating proteins[31]. Many proteins form foci in response to DNA damage-producing treatments[32], meaning that the local accumulation of proteins at the DNA damage-contained sites, and thereby the proteins are involved in DNA damage responses and repair.

We analyzed the formation of RPA-1 foci after 6 h and 16 h HU-treatment, inducing collapsed forks, RPA-1 foci were detected in *exd-3(tm2546)* both short and long HU blocks (Figure 7), indicates that binding region of RPA-1 at stalled and collapsed forks.

In addition, post short HU treatment, the arrested cell cycle was recovered normally in N2 and *exd-3(tm2546)* worms (Figure 5A), indicating that EXD-3 seemed not to affect recovery from stalled replication forks. In contrast, recovery from cell cycle arrest induced by prolonged HU exposure was failed in *exd-3(tm2546)* worms (Figure 5B), this result suggests that EXD-3 is required for rescue of collapsed forks. These results suggest that EXD-3 is involved in formation of competent DNA structure for a rescuing process at collapsed replication forks. Also, we consider whether EXD-3 plays a role in of RPA-1 binding in DNA damage response.

In particular, the response of *exd-3(tm2546)* worms after 6 h, 24 h-CPT treatments are same as 6 h, 16 h-HU exposure, respectively. These observations are enough to affirm that EXD-3 is recruited for formation of competent DNA structure once collapsed replication forks induced.

To confirm whether EXD-3 proteins respond to collapsed forks, we analyzed the formation of EXD-3 foci with anti-EXD-3 antibody after prolonged HU treatment. N2 germline nuclei containing EXD-3 foci were observed after the treatment (Figure 9). In contrast, no foci were observed in *exd-3* mutants. This result suggests that EXD-3 proteins engage in response to or processing collapsed forks.

1	5'	_____	
2		_____	5'
3	5'	_____	
5		_____	5'
		THF	
		A	
4	5'	_____	
5		_____	5'
		dU	
		G	

*****, ³²P labeling

Table 1. List of oligomers.

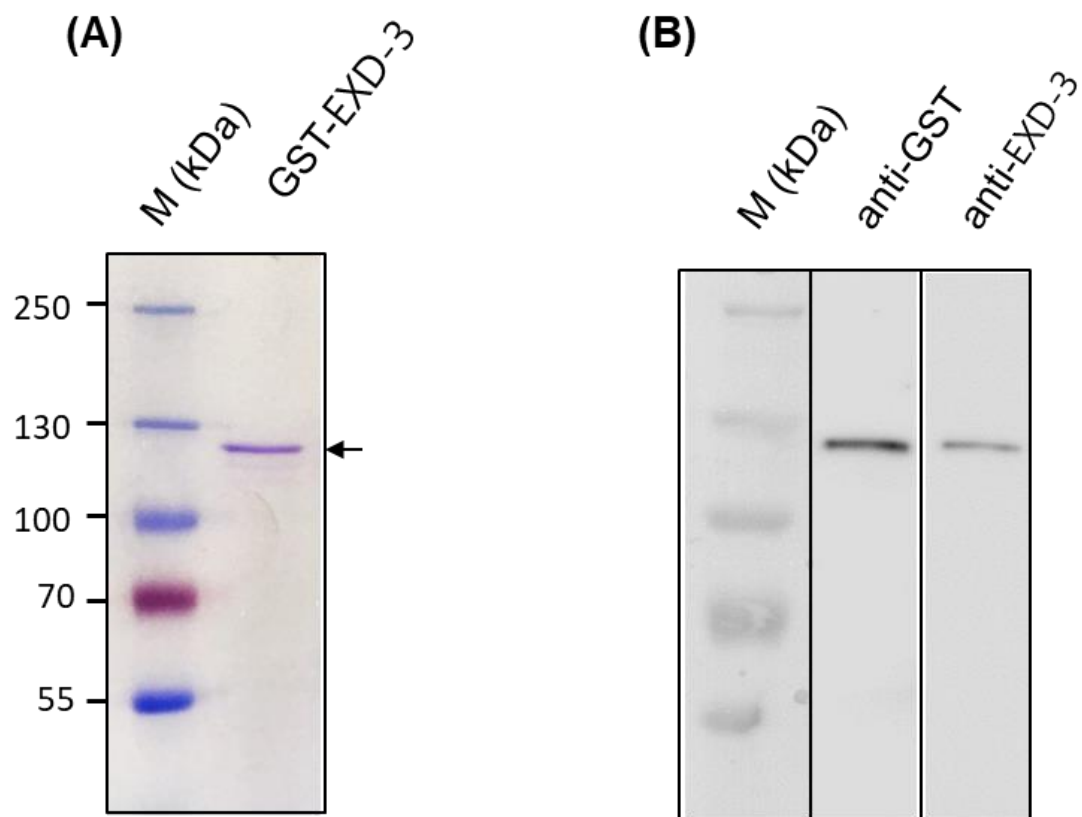


Figure 1. Purification of Recombinant EXD-3 protein.

(A) SDS-PAGE analysis of purified EXD-3. M(kDa), relative molecular mass markers (M kDa), GST-fusion EXD-3 (1 μ g).

(B) Western blot analysis of EXD-3. EXD-3 was separated by SDS-PAGE and subjected to Western Blot analysis using anti-GST or anti- EXD-3 antibodies followed by detection with horse radish peroxidase (Pierce West Pico).

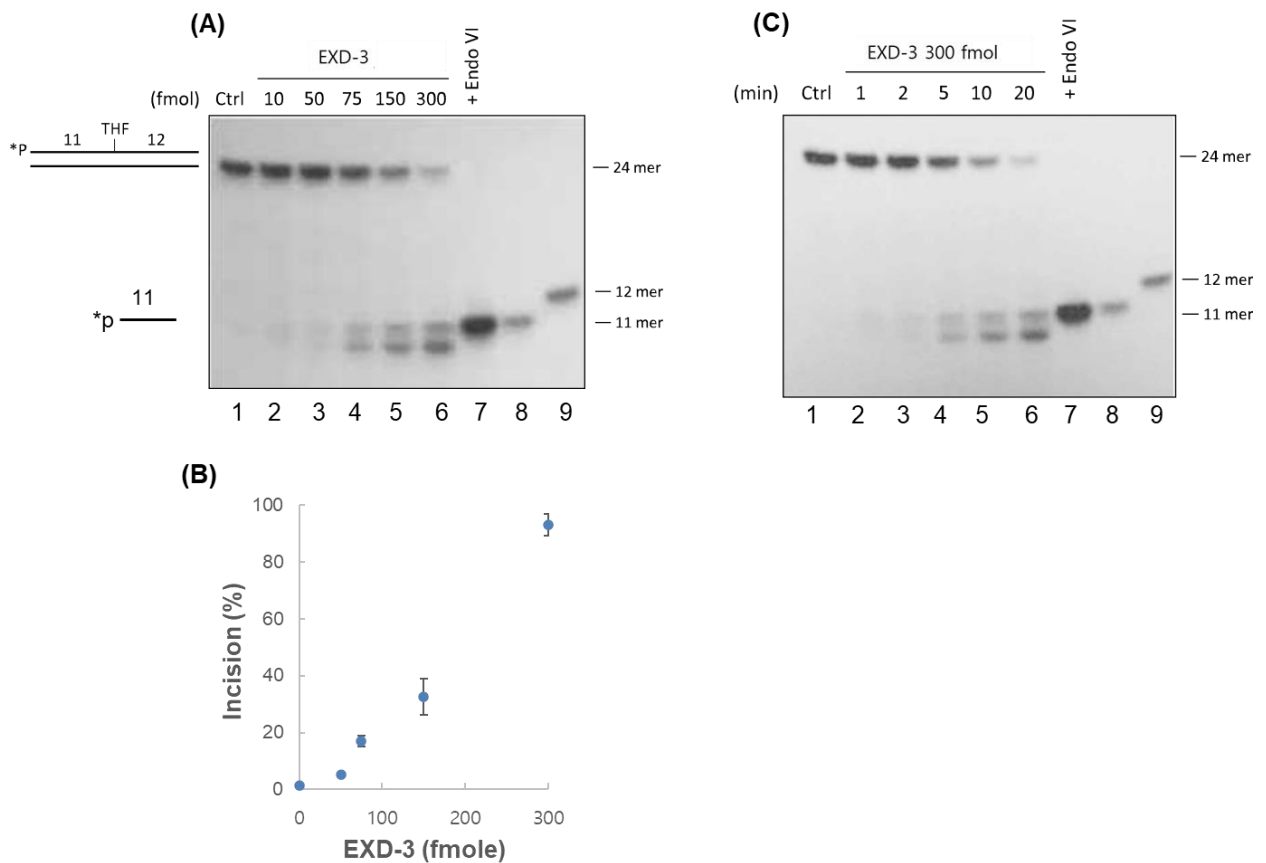


Figure 2. Enzyme activity of EXD-3.

(A) Nicking activity of EXD-3 on THF-AP site

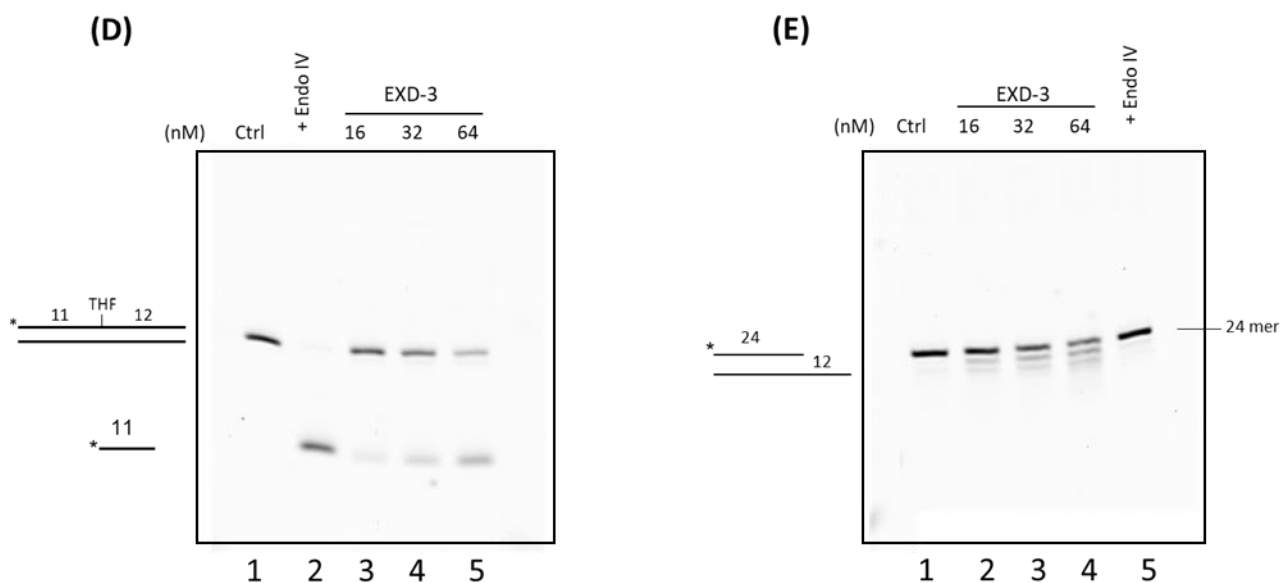
Duplex DNA (24-mer) containing THF-AP site and the size of product is displayed. The substrates (10 fmol) were incubated with EXD-3 at 37°C for 30 min in buffer AP (100 mM Tris/HCl at pH 7.0 and 5 mM MgCl₂). Reaction products were separated by 8 M urea-17% PAGE and the DNA bands were visualized by autoradiography.

Lane 1, no protein added; lanes 2-6, the indicated amounts (fmole) of EXD-3 added; lane 7, with *E. coli* Endo IV (#U); lanes 8 and 9, 11-mer and 12-mer size makers, respectively.

(B) Quantitation of incision of THF AP site by EXD-3 Three independent experiments of (A) were performed and quantitated.

(C) Time-course reaction of EXD-3 nicking activity.

The THF-AP site contained substrates (10 fmol) were incubated EXD-3 (300 fmol) for the indicated times. Lane 1, no protein added; lanes 2-6, for the indicated times (min); lane 7, with *E. coli* Endo IV (#U); lanes 8 and 9, 11-mer and 12-mer size makers, respectively.



(D) AP endonuclease activity of mutant EXD-3 (E452A). Duplex DNA (24-mer) containing THF-AP site and the size of product are displayed. The substrates (100 fmol) were incubated with EXD-3 (E452A) at 37°C for 20 min in buffer AP (40 mM Tris (pH 8.0), 4 mM MgCl₂, 5 mM DTT, 0.1 mg/ml BSA(NEB), 10% glycerol). Reaction products were separated by 18% urea PAGE and the DNA bands were visualized by autoradiography.

Lane 1, no protein added; lane 2, with *E. coli* Endo IV (0.5U); lanes 3-5, the indicated amounts (16, 32, 64 nM) of EXD-3 (E452A) added.

(E) 3'-5' exonuclease activity of EXD-3 (E452A). Products of reaction between 5' overhang substrates and increasing concentrations of EXD-3 (E452A) are showed. The reactions were performed for 20 min at 37°C.

Lanes 1, no protein added, lanes 2-4, the indicated amounts (16, 32, 64 nM) of EXD-3 (E452A) added; lane 5, with *E. coli* Endo IV (0.5U).

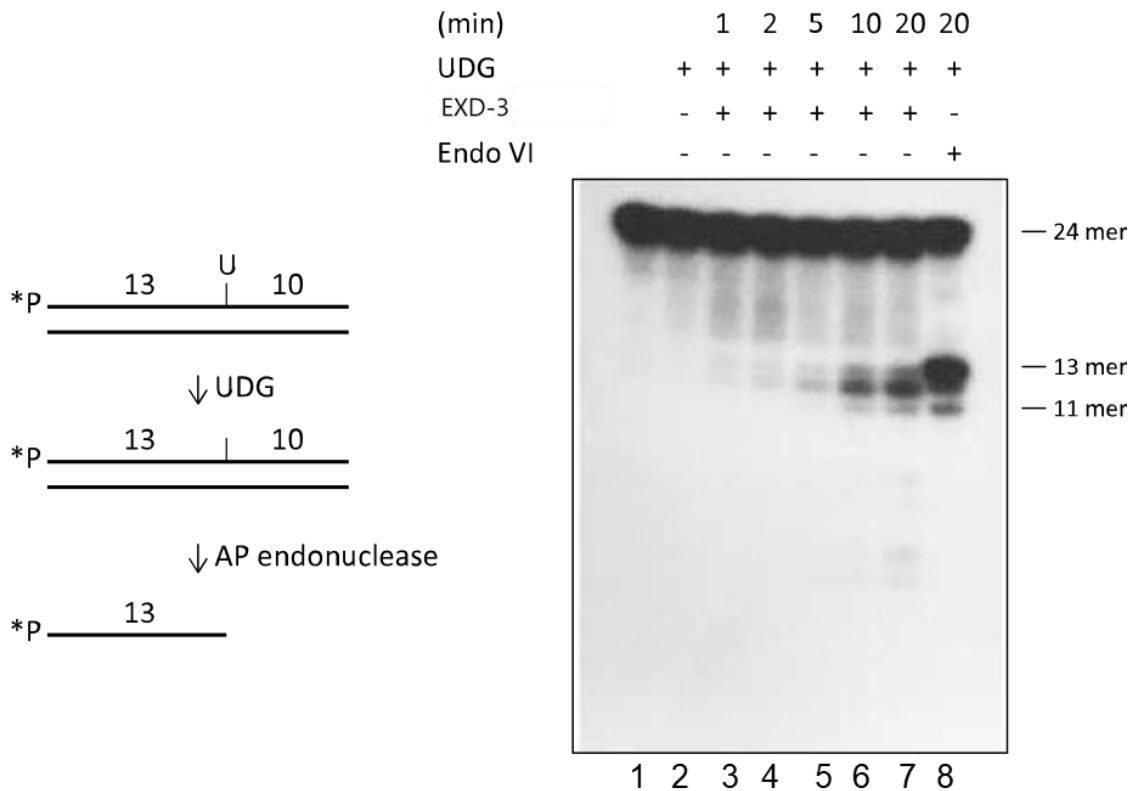


Figure 3. Nicking activity of EXD-3 on a natural abasic site

Duplex DNA (24-mer) containing a U-G pair treated with *E. coli* UDG, leaving an intact AP site. dU is at 14-nt from 5'-end. The resulting AP-containing DNA (1.5 nM) was incubated with EXD-3 (lanes 2-7). or *E. coli* Endo IV (lane 8). Reaction products were separated by 8 urea-17% PAGE and the DNA bands were visualized by autoradiography. The lengths of the fragments are indicated on the right side of the gel.

Lane 1, no protein added; lane 2, with UDG (0.5 U); lanes 3-7, for the indicated times with EXD-3 (300 fmol); Lane 8, *E. coli* Endo IV (0.5 U), producing a 13-mer product.

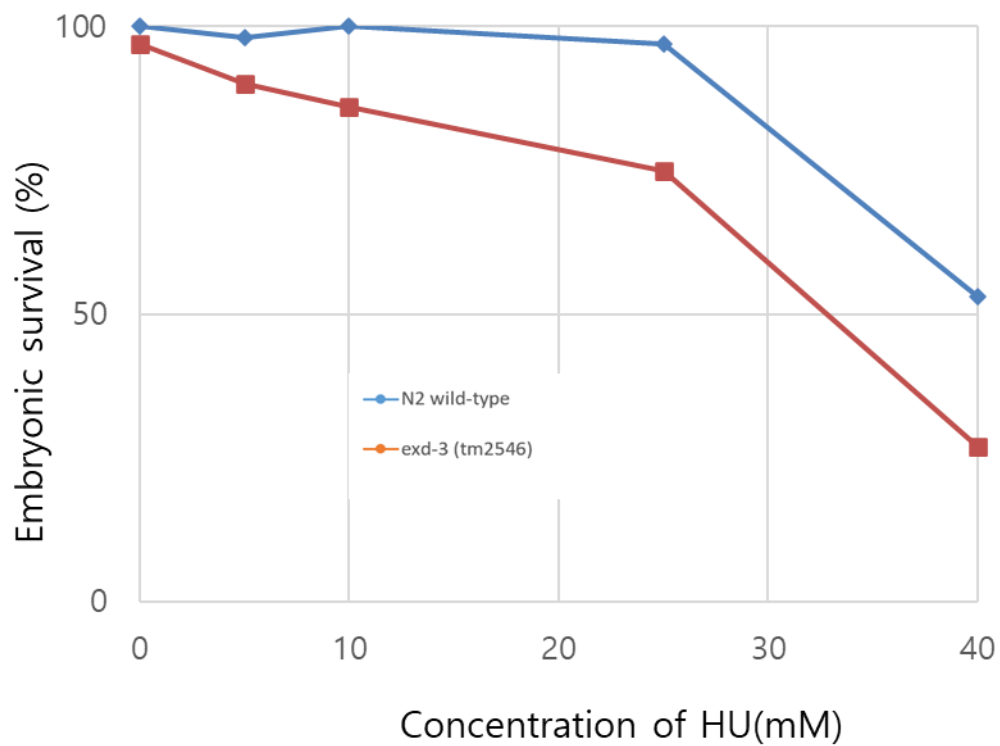
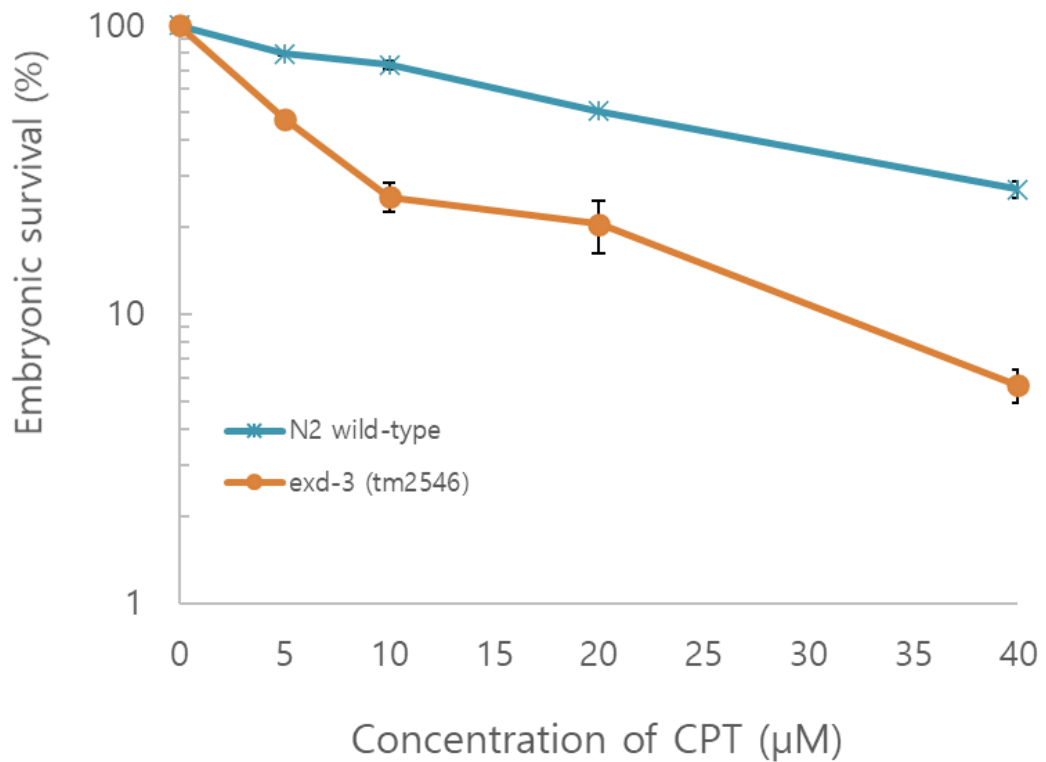


Figure 4. Embryonic survival of *exd-3(tm2546)*

(A) *exd-3(tm2546)* mutant is sensitive to hydroxyurea (HU). L4-stage of N2 and *exd-3(tm2546)* were treated with HU for 16 h and they were placed to HU-free plates to lay eggs for 3 h. The number of total laid eggs (200-300) was counted and post incubated at 20°C for 24 hours, the number of unhatched eggs was also quantified. The error bars indicate the standard errors of the means from three independent experiments.



(B) *C.elegans* *exd-3(tm2546)* is sensitive to Camptothecin (CPT)-induced replication fork stalling.

L4-stage of N2 and *exd-3(tm2546)* were treated with CPT for 24 h and they were transferred to CPT-free plates to lay eggs for 3 h.

After 24 h incubation at 20°C, the embryonic survival was calculated by dividing the number of hatched eggs by the number of total laid eggs (200-300). The error bars represent the mean \pm standard deviation from three independent experiments.

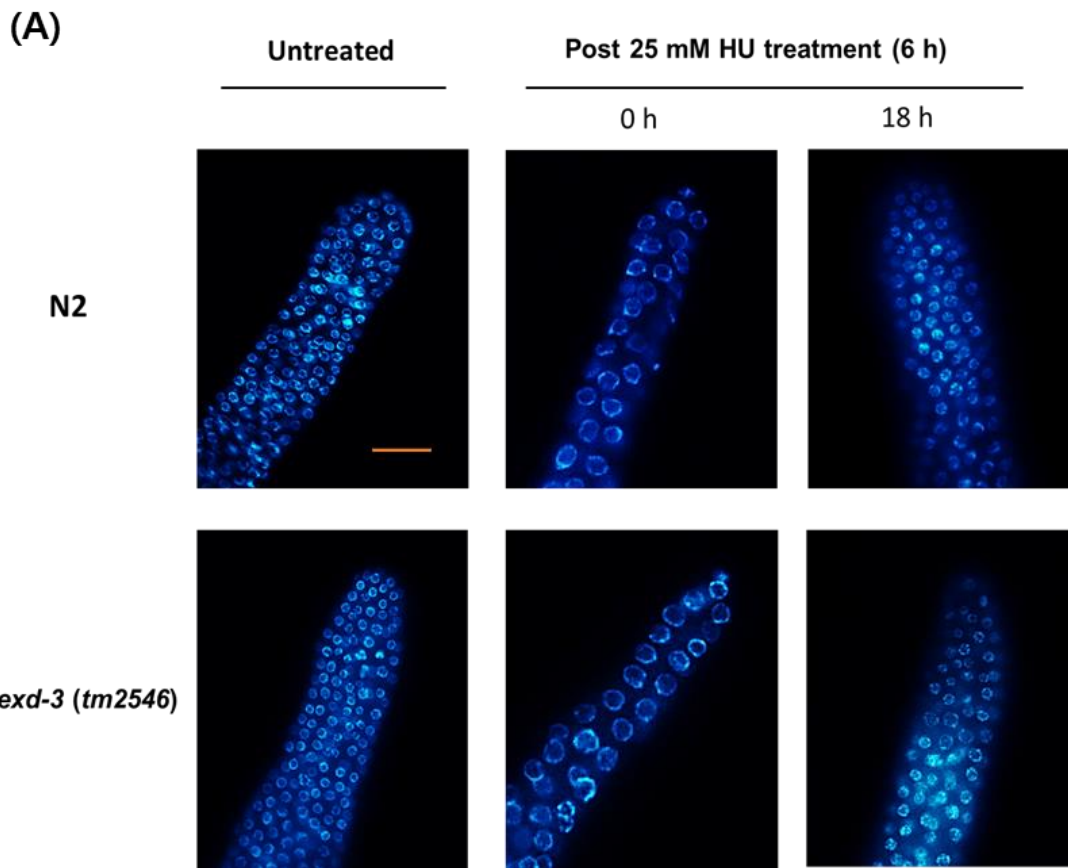
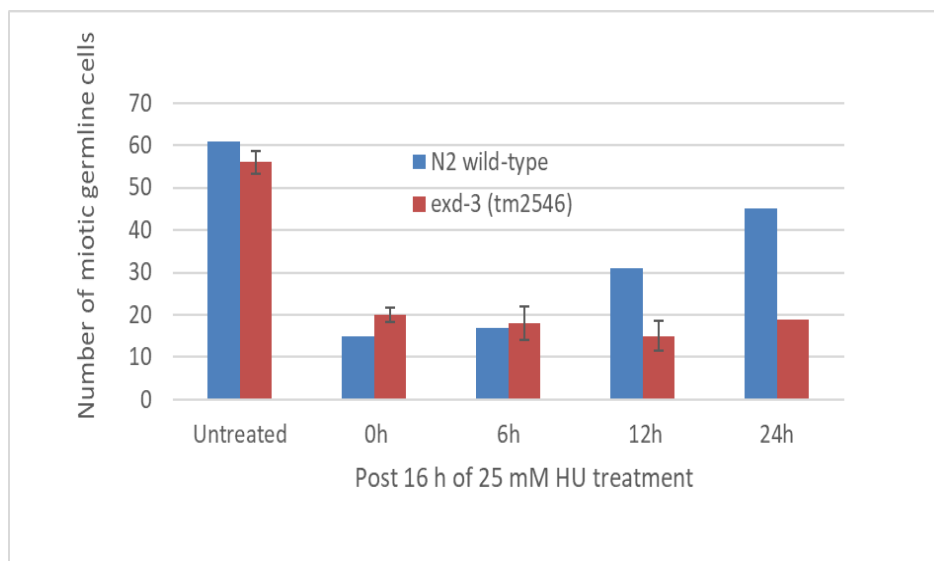
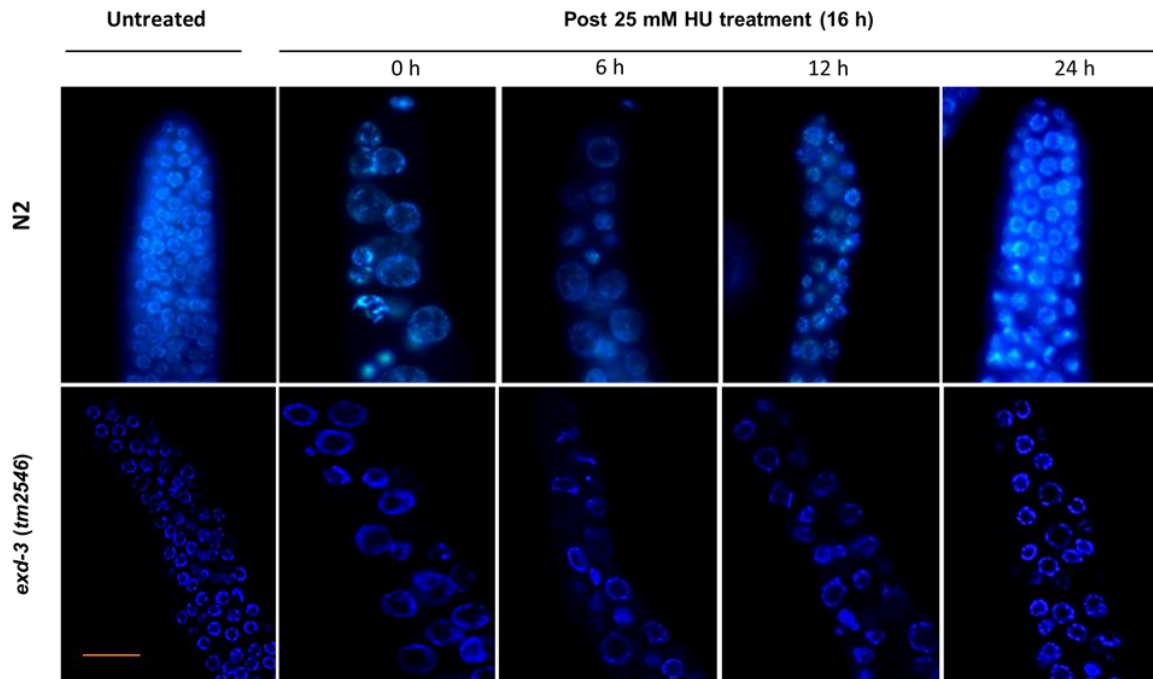


Figure 5. Recovery from cell cycle arrest post HU treatment.

(A) Representative images of fixed germ cells of indicated genotypes stained with DAPI. L4 worms were transferred to NGM plates after a 6-h exposure to HU and allowed recovery for indicated times. The gonads were dissected and collected from 20 worms at 18 h post HU-treatment and stained with DAPI. Magnification bars, 10 μ m.

(B)



(B) Representative images of fixed germ cells of indicated genotypes stained with DAPI. L4 worms were transferred to NGM plates after a 16-h exposure to HU and allowed recovery for 24-h. Gonads were dissected from 20 worms at the indicated times post HU-treatment and stained with DAPI. Germ cells in the mitotically proliferating region of gonads (within 50 x 20 μm of the tip cell) were counted under a fluorescence microscope. Error bars indicate standard errors of means of 10 worms of each genotype.

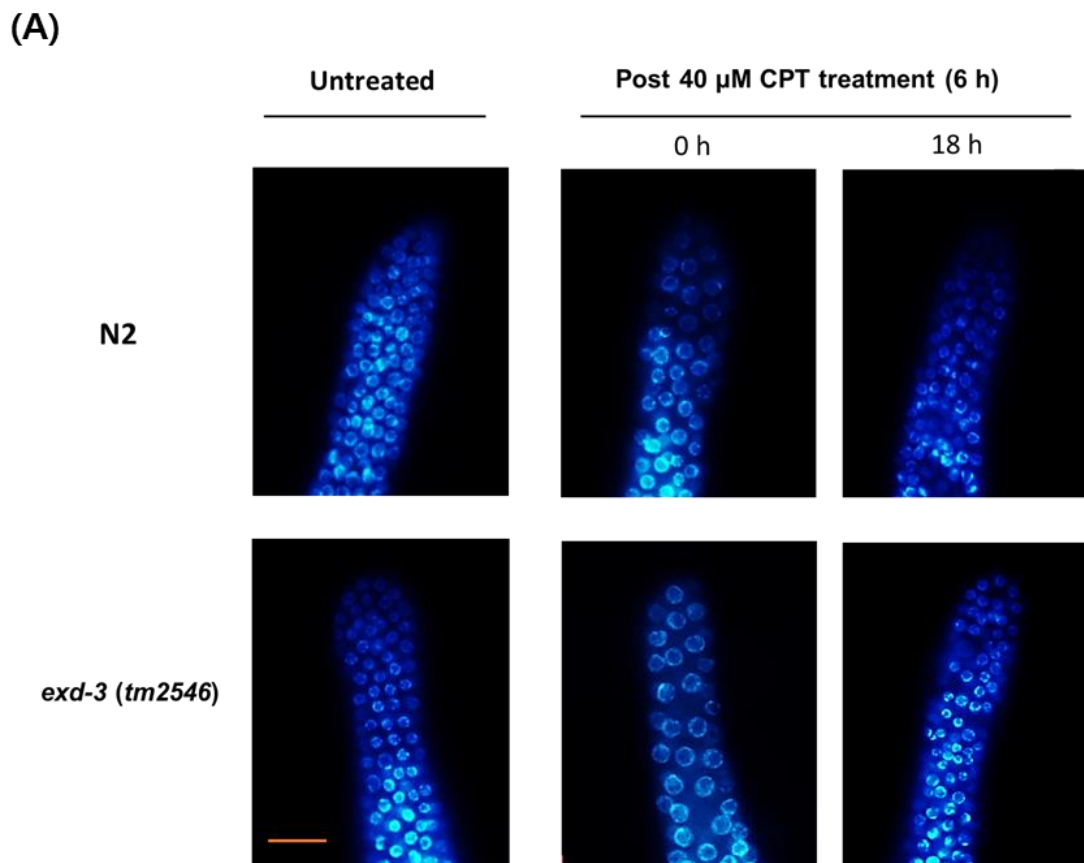
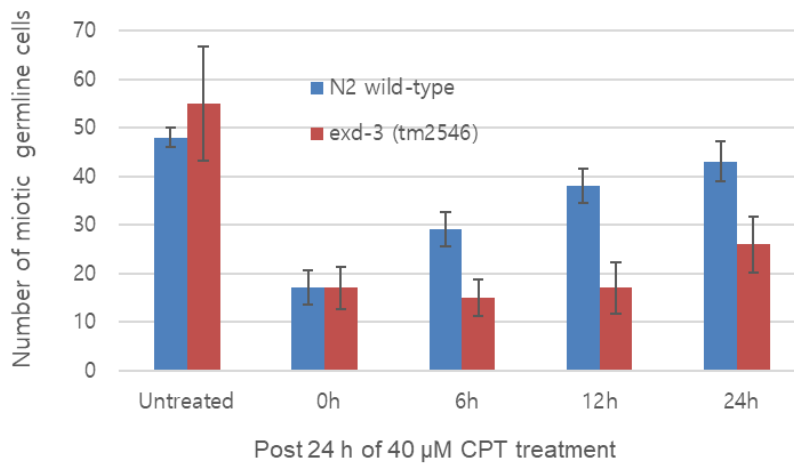
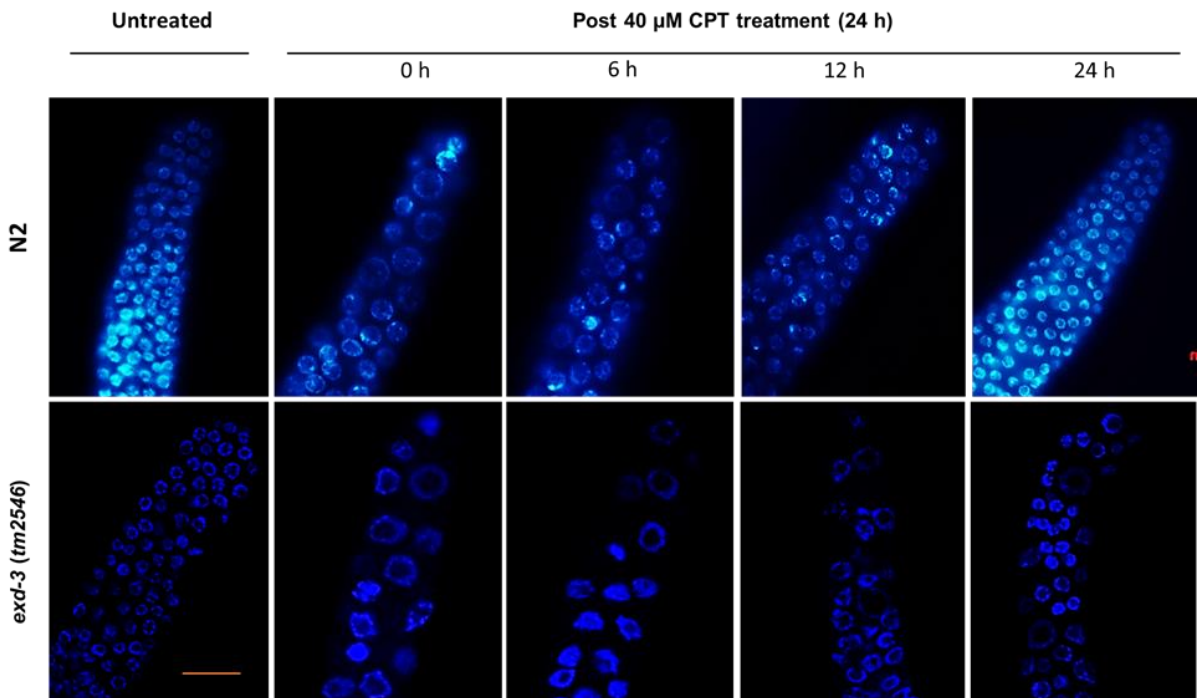


Figure 6. Recovery from cell cycle arrest post CPT-treatment

(A) Representative images of fixed germ cells of indicated genotypes stained with DAPI. L4 worms were transferred to NGM plates after a 6-h exposure to CPT and allowed recovery for indicated times. Gonads were dissected from the worms at 18-h post CPT-treatment and stained with DAPI. Magnification bars, 10 μ m.

(B)



(B) Representative images of fixed germ cells of indicated genotypes stained with DAPI. L4 worms were transferred to NGM plates after a 24-h exposure to CPT and allowed recovery for indicated times. Gonads were dissected from the 20 worms at the indicated times post CPT-treatment and stained with DAPI. Magnification bars, 10 μm. Germ cells in the mitotically proliferating region of gonads (within 50 x 20 μm of the tip cell) were counted under a fluorescence microscope. Error bars indicate standard errors of means of 10 worms of each genotype.

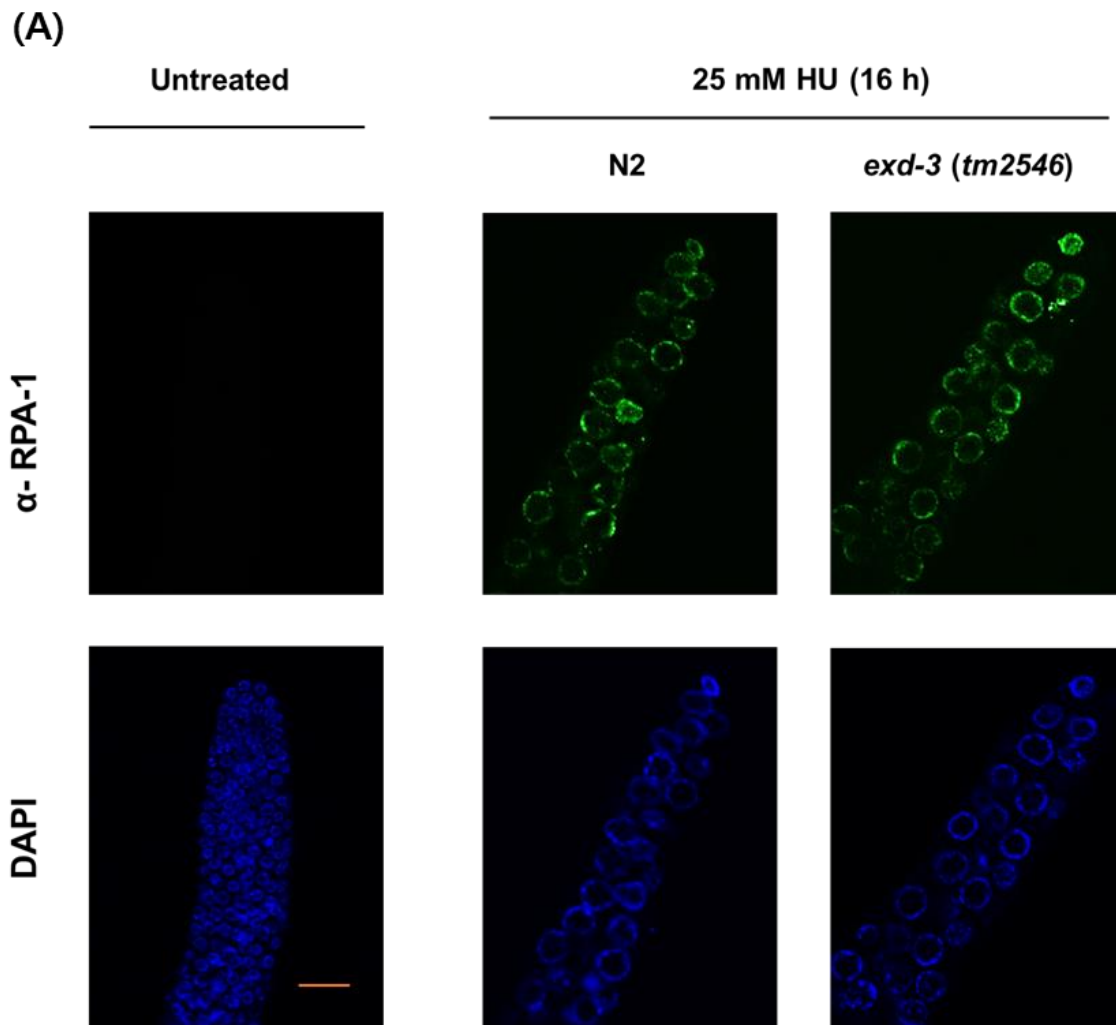
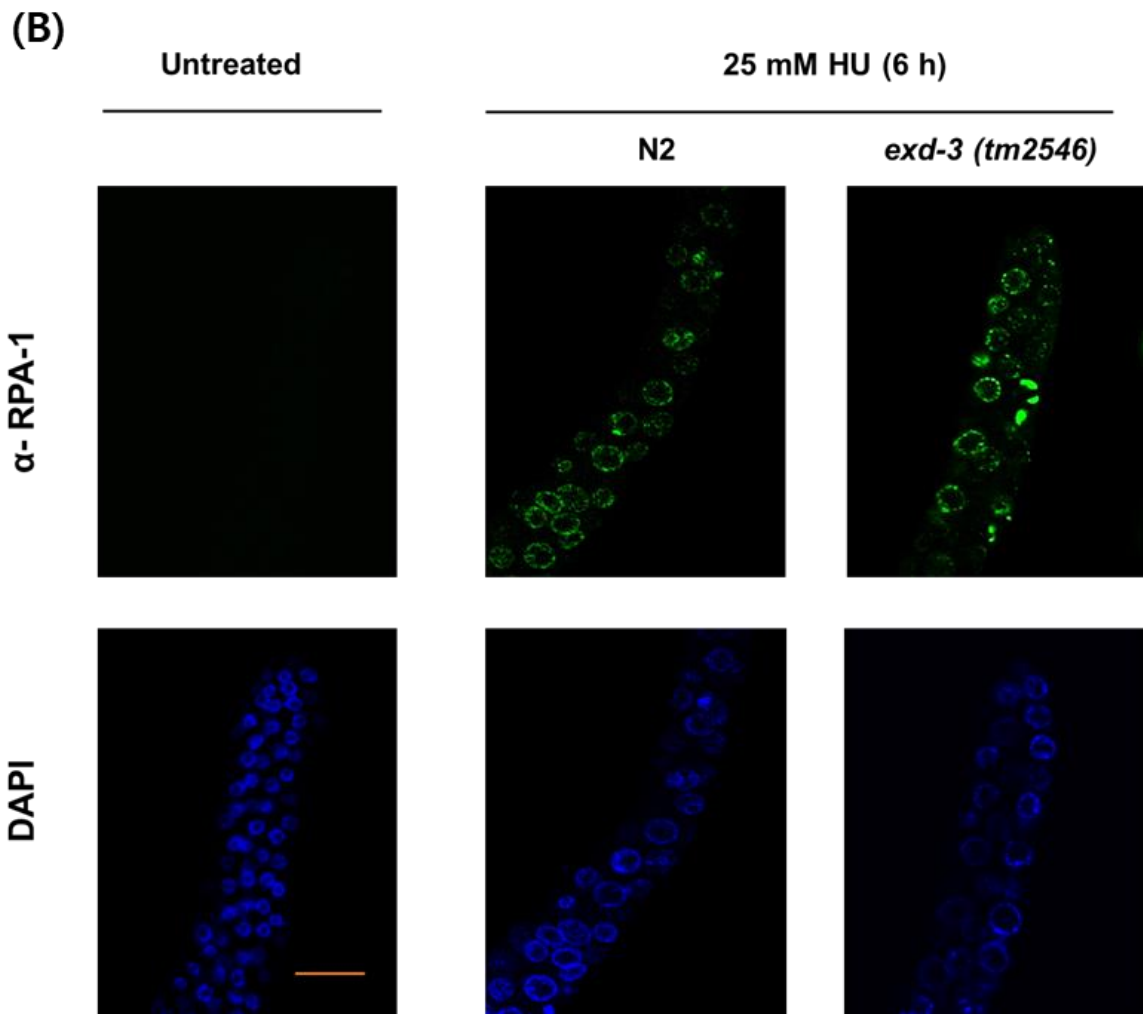


Figure 7. *exd-3(tm2546)* worms respond to HU-induced DNA damage.

(A) L4 worms were dissected after a 16-h exposure to HU and then the gonads were immunostained with anti-RPA-1 antibody and stained with DAPI. Magnification bars, 10 μ m.



(B) L4 worms of N2 and *exd-3(tm2546)* were dissected after a 6-h exposure to HU and then the gonads were immunostained with anti-RPA-1 antibody and stained with DAPI. Magnification bars, 10 μ m.

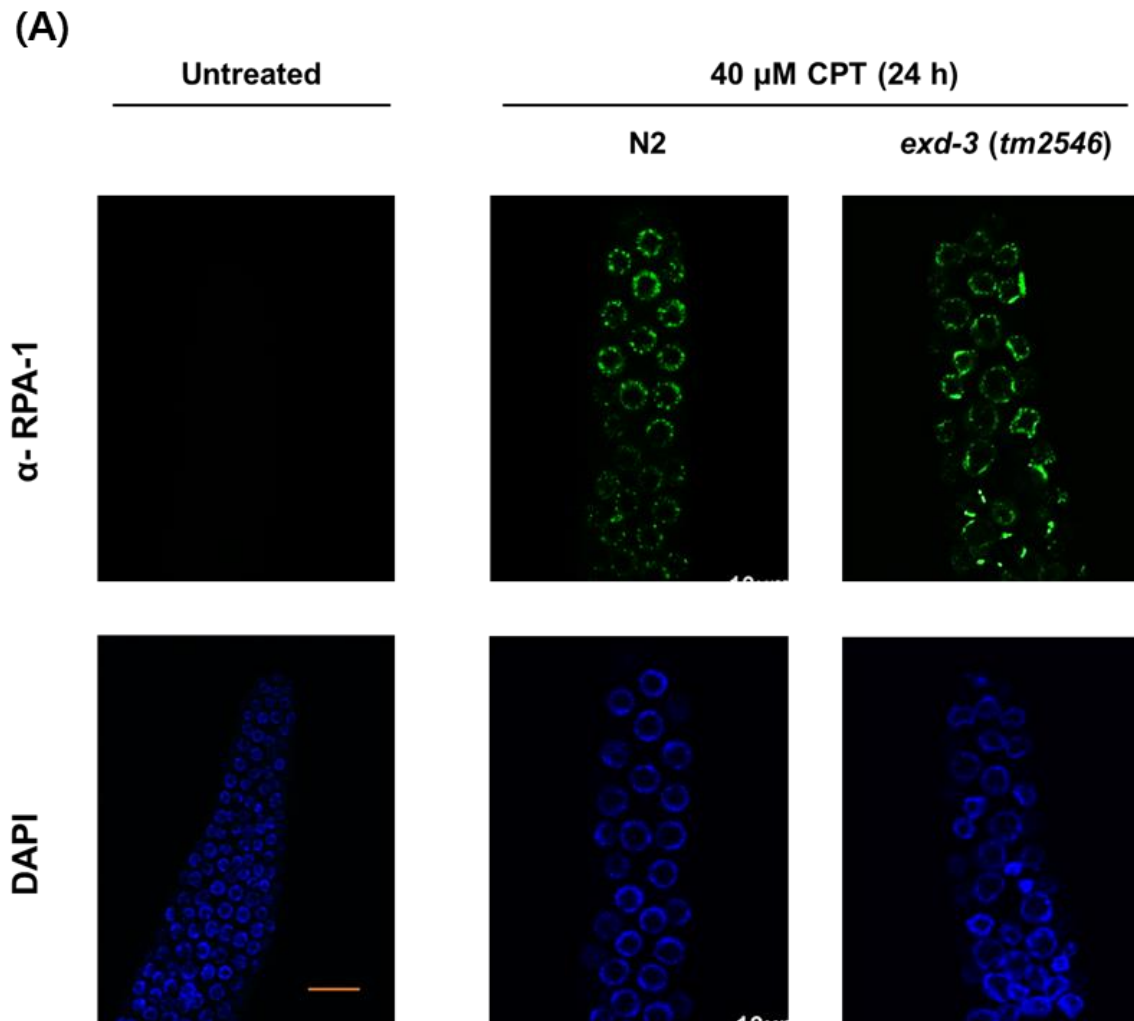
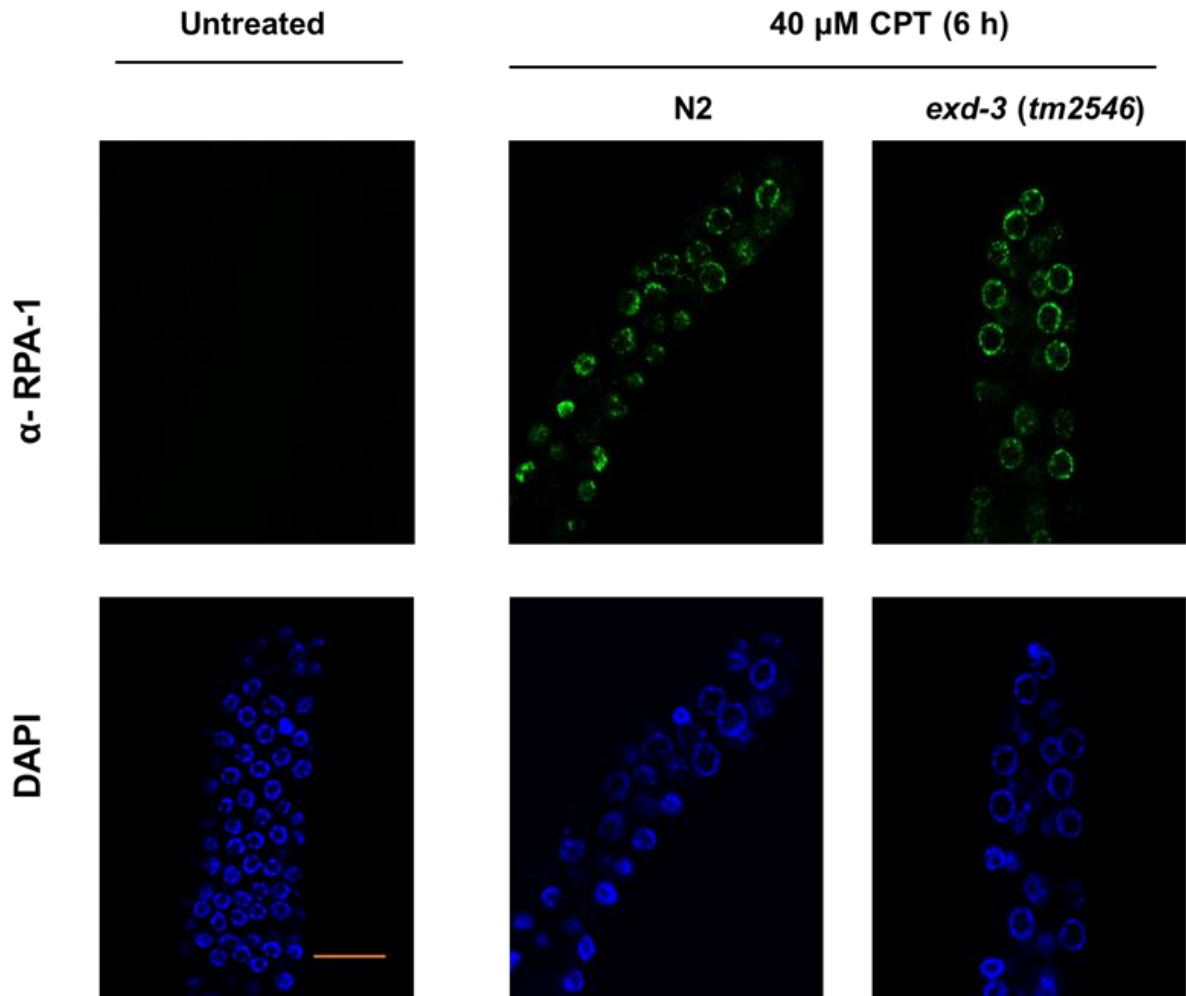


Figure 8. *exd-3(tm2546)* worms respond to CPT-induced DNA damage.

(A) L4 worms of N2 were dissected after a 24-h exposure to CPT and then the gonads were immunostained with anti-RPA-1 antibody and stained with DAPI. Magnification bars, 10 μ m.

(B)



(B) L4 worms of N2 and *exd-3(tm2546)* were dissected after a 6-h exposure to CPT and then the gonads were immunostained with anti-RPA-1 antibody and stained with DAPI.

Magnification bars, 10 μm.

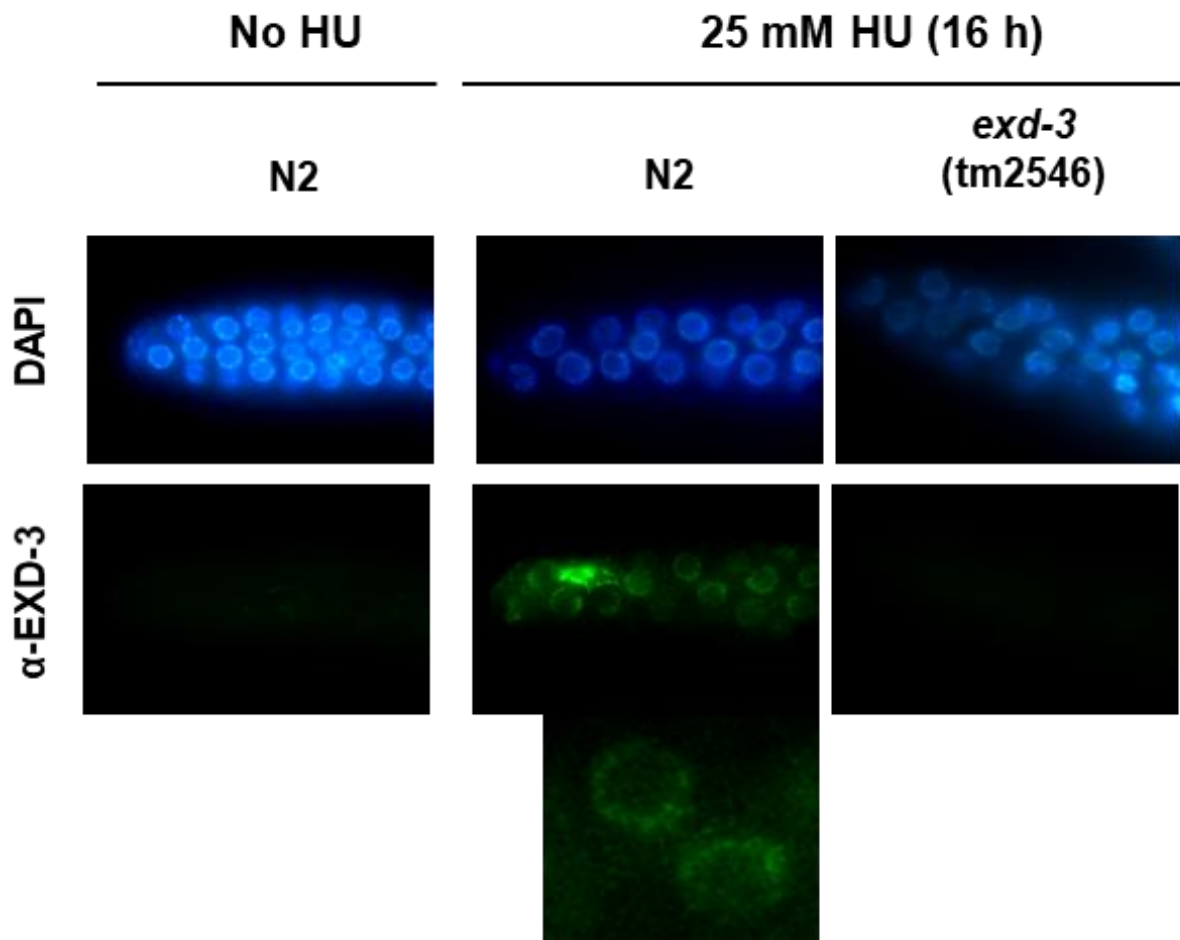


Figure 9. Formation of EXD-3 foci after HU treatment

Representative images of fixed germ cells of indicated genotypes.

L4 worms of N2 or *exd-3(tm2546)* were dissected after a 16h-exposure to HU and then the gonads were immunostained with anti- α -EXD-3 antibody and stained with DAPI

Discussion

We have identified a new *C. elegans* protein with AP endonuclease and exonuclease activities. The protein has an exonuclease domain—a domain with sequence similarities to human EXD3 (exonuclease 3'-5' domain containing 3) domain and human WRN exonuclease domain and thus is predicted to have 3'-5' exonuclease activity. However, Although EXD-3 does not have a similar domain to two identified *C. elegans* AP endonucleases, EXD-3 has AP endonuclease activity.

The EXD-3 incised duplex DNA at THF-AP site and natural AP site. In addition, EXD-3 showed 3'–5' exonucleolytic degradation of the incised AP site, producing smaller products. However, such degradation was not detected in two *C. elegans* AP endonucleases [14;15]. This exonuclease activity may use the same active site as AP endonuclease. This sequential action was also detected in PolX_{Bs} [22] and human PALF [23]. If EXD-3 preferentially binds to AP residue, a binding to the 3' end consequently would be prevented. Thus, the presence of an abasic site in a linear DNA may hinder exonucleolytic degradation of the 3' ends. Single strand nick generated by AP endonuclease would recruit other protein, such as PARP1 which is involved in single strand break repair [33]. Human PALF protein has shown to interact with and activates PARP1 [23]. Thus, it may possible for EXD-3 to regulate other proteins in response to and repair DNA damage.

Interestingly, new AP endonucleases that do not belong to two typical AP endonuclease families have been reported. *Bacillus subtilis* has two AP endonucleases and one extra AP endonuclease which is a part of DNA polymerase X (PolX_{Bs}) [22]. The AP endonucleas of PolX_{Bs} is genetically linked to exonuclease. In humans, two AP endonucleases belong to only Exo III family and a human PALF protein with an FHA (forkhead-associated) domain and a zinc-finger-like CYR (cysteine–tyrosine–arginine) motif has AP endonuclease activity [23]. However, EXD-3 does not have amino acid similarities to PolX_{Bs} and human PALF and is different from two *C. elegans* AP endonucleases.

This study shows that *exd-3(tm2546)* mutants did not resume cell cycle progression from

stalled fork-induced cell cycle arrest. However, *exd-3* mutants showed a normal HU-induced cell cycle arrest. Prolonged HU treatment for 16 to 24 h leads to fork collapse which must be rescued [34]. Cleavage of stalled fork causes the fork to collapse and consequently generate a single-ended DSB. Then, new origin firing produces another single-ended DSB[35;36]. At the DSB, replication is not restarted, but instead, DSB is repaired by homologous recombination involving double Holiday junction, synthesis-dependent strand annealing (SDSA) or nonhomologous end joining (NHEJ)[31;37]. Thus, no recovery of *exd-3* mutants after prolonged HU treatment suggests that accumulated DSBs may not be repaired or some component required for terminating checkpoint-mediated arrest after repair may be lost. RPA-ssDNA complexes that arise during replication stress or following DNA damage recruit ATR which induces S-phase arrest through activating CHK1 kinase[38-40]. Short treatments of HU or CPT can induce S-phase arrest through accumulation of RPA at stalled forks and Long HU blocks induce also accumulation of RPA and DSB repair proteins. [31]. In this study, RPA-1 foci were formed after long HU blocks (25 mM, 16 h) in N2, consistent with the result obtained in mammalian cells[31] and a previously published observation in *C. elegans*[41]. In contrast, *exd-3* mutants showed that they cannot recovery after long exposure to HU and CPT and that cell cycle arrest in the mutants was not recovered. This observation suggests that there may be no ssDNA region at DSBs for RPA-1 to bind and thereby rescue of collapsed replication may not be further processed since DSBs at collapsed replication forks are repaired by HR which requires RPA-1 and RAD-51[31]. Therefore, this study suggests that EXD-3 may be required for producing DNA structure competent for RPA-1 foci formation at collapsed replication forks or for rescuing collapsed replication forks.

The involvement of EXD-3 in the cellular response to DSBs is further suggested by its foci formation after prolonged HU treatment. Since DSBs are induced at blocked replication forks, foci formation of EXD-3 indicates that EXD-3 may be recruited to DSBs by other proteins or recognize DSBs. Human PALF containing AP endonuclease activity is also reported to be involved in DSB response[23]. Knock-down of *exd-3* expression did not have any influence on cell survival after *tert*-butyl hydroperoxide (organic peroxide), inducing oxidative stress, in our experimental conditions (data not shown). Thus, EXD-3 may be involved in various DSB responses. However, its real function in DSB response remains to be further elucidated.

Here, we have described a novel protein with AP endonuclease activity and response to replication fork-associated DNA damage.

References

- [1] Krokan HE & Bjoras M (2013) Base excision repair. *Cold Spring Harb. Perspect. Biol.*, 5, a012583.
- [2] Lindahl T (1993) Instability and decay of the primary structure of DNA. *Nature*, 362, 709-715.
- [3] Lindahl T & Nyberg B (1972) Rate of depurination of native deoxyribonucleic acid. *Biochemistry*, 11, 3610-3618.
- [4] Boiteux S & Guillet M (2004) Abasic sites in DNA: repair and biological consequences in *Saccharomyces cerevisiae*. *DNA Repair (Amst)*, 3, 1-12.
- [5] Loeb LA & Preston BD (1986) Mutagenesis by apurinic/apyrimidinic sites. *Annu. Rev. Genet.*, 20, 201-230.
- [6] Auerbach P, Bennett RA, Bailey EA, Krokan HE, & Demple B (2005) Mutagenic specificity of endogenously generated abasic sites in *Saccharomyces cerevisiae* chromosomal DNA. *Proc. Natl. Acad. Sci. U. S. A.*, 102, 17711-17716.
- [7] Daley JM, Zakaria C, & Ramotar D (2010) The endonuclease IV family of apurinic/apyrimidinic endonucleases. *Mutat. Res.*, 705, 217-227.
- [8] Mol CD, Hosfield DJ, & Tainer JA (2000) Abasic site recognition by two apurinic/apyrimidinic endonuclease families in DNA base excision repair: the 3' ends justify the means. *Mutat. Res.*, 460, 211-229.
- [9] Miertzschke M & Greiner-Stoffele T (2003) The xthA gene product of *Archaeoglobus fulgidus* is an unspecific DNase. *Eur. J. Biochem.*, 270, 1838-1849.

- [10] Levin JD, Shapiro R, & Demple B (1991) Metalloenzymes in DNA repair. *Escherichia coli* endonuclease IV and *Saccharomyces cerevisiae* Apn1. *J. Biol. Chem.*, 266, 22893-22898.
- [11] Nakamura N, Morinaga H, Kikuchi M, Yonekura S, Ishii N, Yamamoto K, Yonei S, & Zhang QM (2008) Cloning and characterization of uracil-DNA glycosylase and the biological consequences of the loss of its function in the nematode *Caenorhabditis elegans*. *Mutagenesis*, 23, 407-413.
- [12] Morinaga H, Yonekura S, Nakamura N, Sugiyama H, Yonei S, & Zhang-Akiyama QM (2009) Purification and characterization of *Caenorhabditis elegans* NTH, a homolog of human endonuclease III: essential role of N-terminal region. *DNA Repair (Amst)*, 8, 844-851.
- [13] Shatilla A & Ramotar D (2002) Embryonic extracts derived from the nematode *Caenorhabditis elegans* remove uracil from DNA by the sequential action of uracil-DNA glycosylase and AP (apurinic/aprimidinic) endonuclease. *Biochem. J.*, 365, 547-553.
- [14] Shatilla A, Ishchenko AA, Sapparbaev M, & Ramotar D (2005) Characterization of *Caenorhabditis elegans* exonuclease-3 and evidence that a Mg²⁺-dependent variant exhibits a distinct mode of action on damaged DNA. *Biochemistry*, 44, 12835-12848.
- [15] Shatilla A, Leduc A, Yang X, & Ramotar D (2005) Identification of two apurinic/aprimidinic endonucleases from *Caenorhabditis elegans* by cross-species complementation. *DNA Repair (Amst)*, 4, 655-670.
- [16] Asagoshi K, Lehmann W, Braithwaite EK, Santana-Santos L, Prasad R, Freedman JH, Van HB, & Wilson SH (2012) Single-nucleotide base excision repair DNA polymerase activity in *C. elegans* in the absence of DNA polymerase beta. *Nucleic Acids Res.*, 40, 670-681.
- [17] Yang X, Fan J, Ishchenko AA, Patel D, Sapparbaev MK, & Ramotar D (2012) Functional characterization of the *Caenorhabditis elegans* DNA repair enzyme APN-1. *DNA Repair (Amst)*, 11, 811-822.

- [18] Masson JY, Tremblay S, & Ramotar D (1996) The *Caenorhabditis elegans* gene CeAPN1 encodes a homolog of *Escherichia coli* and yeast apurinic/aprimidinic endonuclease. *Gene*, 179, 291-293.
- [19] Hadi MZ, Ginalski K, Nguyen LH, & Wilson DM, III (2002) Determinants in nuclease specificity of Ape1 and Ape2, human homologues of *Escherichia coli* exonuclease III. *J. Mol. Biol.*, 316, 853-866.
- [20] Carpenter EP, Corbett A, Thomson H, Adacha J, Jensen K, Bergeron J, Kasampalidis I, Exley R, Winterbotham M, Tang C, Baldwin GS, & Freemont P (2007) AP endonuclease paralogues with distinct activities in DNA repair and bacterial pathogenesis. *EMBO J.*, 26, 1363-1372.
- [21] Murphy TM, Belmonte M, Shu S, Britt AB, & Hatteroth J (2009) Requirement for abasic endonuclease gene homologues in *Arabidopsis* seed development. *PLoS. One.*, 4, e4297.
- [22] Banos B, Villar L, Salas M, & de VM (2010) Intrinsic apurinic/aprimidinic (AP) endonuclease activity enables *Bacillus subtilis* DNA polymerase X to recognize, incise, and further repair abasic sites. *Proc. Natl. Acad. Sci. U. S. A.*, 107, 19219-19224.
- [23] Kanno S, Kuzuoka H, Sasao S, Hong Z, Lan L, Nakajima S, & Yasui A (2007) A novel human AP endonuclease with conserved zinc-finger-like motifs involved in DNA strand break responses. *EMBO J.*, 26, 2094-2103.
- [24] Hyun M, Park S, Kim E, Kim DH, Lee SJ, Koo HS, Seo YS, & Ahn B (2012) Physical and functional interactions of *Caenorhabditis elegans* WRN-1 helicase with RPA-1. *Biochemistry*, 51, 1336-1345.
- [25] Huang S, Beresten S, Li B, Oshima J, Ellis NA, & Campisi J (2000) Characterization of

the human and mouse WRN 3'→5' exonuclease. *Nucleic Acids Res.*, 28, 2396-2405.

[26] Hosfield DJ, Guan Y, Haas BJ, Cunningham RP, & Tainer JA (1999) Structure of the DNA repair enzyme endonuclease IV and its DNA complex: double-nucleotide flipping at abasic sites and three-metal-ion catalysis. *Cell*, 98, 397-408.

[27] Lindahl T (1974) An N-glycosidase from *Escherichia coli* that releases free uracil from DNA containing deaminated cytosine residues. *Proc. Natl. Acad. Sci. U. S. A.*, 71, 3649-3653.

[28] Gartner A, Milstein S, Ahmed S, Hodgkin J, & Hengartner MO (2000) A conserved checkpoint pathway mediates DNA damage--induced apoptosis and cell cycle arrest in *C. elegans*. *Mol. Cell*, 5, 435-443.

[29] Craig AL, Moser SC, Bailly AP, & Gartner A (2012) Methods for studying the DNA damage response in the *Caenorhabditis elegans* germ line. *Methods Cell Biol.*, 107, 321-352.

[30] Berniak K, Rybak P, Bernas T, Zarebski M, Biela E, Zhao H, Darzynkiewicz Z, & Dobrucki JW (2013) Relationship between DNA damage response, initiated by camptothecin or oxidative stress, and DNA replication, analyzed by quantitative 3D image analysis. *Cytometry A*, 83, 913-924.

[31] Petermann E, Orta ML, Issaeva N, Schultz N, & Helleday T (2010) Hydroxyurea-stalled replication forks become progressively inactivated and require two different RAD51-mediated pathways for restart and repair. *Mol. Cell*, 37, 492-502.

[32] Stiff T, O'Driscoll M, Rief N, Iwabuchi K, Lobrich M, & Jeggo PA (2004) ATM and DNA-PK function redundantly to phosphorylate H2AX after exposure to ionizing radiation. *Cancer Res.*, 64, 2390-2396.

[33] Abbotts R & Wilson DM, III (2017) Coordination of DNA single strand break repair. *Free Radic. Biol. Med.*, 107, 228-244.

[34] Saintigny Y, Delacote F, Vares G, Petitot F, Lambert S, Averbeck D, & Lopez BS (2001) Characterization of homologous recombination induced by replication inhibition in mammalian cells. *EMBO J.*, 20, 3861-3870.

[35] Hanada K, Budzowska M, Davies SL, van DE, Onizawa H, Beverloo HB, Maas A, Essers J, Hickson ID, & Kanaar R (2007) The structure-specific endonuclease Mus81 contributes to replication restart by generating double-strand DNA breaks. *Nat. Struct. Mol. Biol.*, 14, 1096-1104.

[36] Mayle R, Campbell IM, Beck CR, Yu Y, Wilson M, Shaw CA, Bjergbaek L, Lupski JR, & Ira G (2015) DNA REPAIR. Mus81 and converging forks limit the mutagenicity of replication fork breakage. *Science*, 349, 742-747.

[37] Alexander JL & Orr-Weaver TL (2016) Replication fork instability and the consequences of fork collisions from rereplication. *Genes Dev.*, 30, 2241-2252.

[38] Lopes M, Cotta-Ramusino C, Pelliccioli A, Liberi G, Plevani P, Muzi-Falconi M, Newlon CS, & Foiani M (2001) The DNA replication checkpoint response stabilizes stalled replication forks. *Nature*, 412, 557-561.

[39] Tercero JA & Diffley JF (2001) Regulation of DNA replication fork progression through damaged DNA by the Mec1/Rad53 checkpoint. *Nature*, 412, 553-557.

[40] Zou L & Elledge SJ (2003) Sensing DNA damage through ATRIP recognition of RPA-ssDNA complexes. *Science*, 300, 1542-1548.

[41] Lee SJ, Gartner A, Hyun M, Ahn B, & Koo HS (2010) The *Caenorhabditis elegans* Werner syndrome protein functions upstream of ATR and ATM in response to DNA replication inhibition and double-strand DNA breaks. *PLoS. Genet.*, 6, e1000801.